

See discussions, stats, and author profiles for this publication at: <https://www.researchgate.net/publication/6419997>

# Melting and Freezing Behaviors of Prototype Ionic Liquids, 1-Butyl-3-methylimidazolium Bromide and Its Chloride, Studied by Using a Nano-Watt Differential Scanning Calorimeter †

ARTICLE in THE JOURNAL OF PHYSICAL CHEMISTRY B · JUNE 2007

Impact Factor: 3.3 · DOI: 10.1021/jp0671852 · Source: PubMed

---

CITATIONS

62

---

READS

105

7 AUTHORS, INCLUDING:



Keiko Nishikawa

Chiba University

217 PUBLICATIONS 3,965 CITATIONS

SEE PROFILE



Ken-ichi Tozaki

Chiba University

68 PUBLICATIONS 561 CITATIONS

SEE PROFILE

# Melting and Freezing Behaviors of Prototype Ionic Liquids, 1-Butyl-3-methylimidazolium Bromide and Its Chloride, Studied by Using a Nano-Watt Differential Scanning Calorimeter<sup>†</sup>

Keiko Nishikawa,<sup>\*,‡</sup> Shaolan Wang,<sup>‡</sup> Hideki Katayanagi,<sup>§</sup> Satoshi Hayashi,<sup>||</sup> Hiro-o Hamaguchi,<sup>||</sup> Yoshikata Koga,<sup>⊥</sup> and Ken-ichi Tozaki<sup>#</sup>

Graduate School of Science and Technology, Chiba University, Yayoi, Inage-ku, Chiba, 263-8522, Japan, Center for Frontier Electronics and Photonics, Chiba University, Yayoi, Inage-ku, Chiba, 263-8522, Japan, Department of Chemistry, School of Science, The University of Tokyo, Hongo, Bunkyo-ku, Tokyo 113-0033, Japan, Department of Chemistry, The University of British Columbia, Vancouver, B.C., Canada V6T 1W5, and Faculty of Education, Chiba University, Yayoi, Inage-ku, Chiba, 263-8522, Japan

Received: October 31, 2006; In Final Form: December 26, 2006

1-Butyl-3-methylimidazolium bromide ([bmim]Br) and its chloride ([bmim]Cl) are representative prototypes of ionic liquids. We investigated the melting and freezing behaviors of [bmim]Br and [bmim]Cl by using a homemade differential scanning calorimeter (DSC) with nano-Watt stability and sensitivity. The measurements were carried out at heating and cooling rates slow enough to mimic quasi-static processes. Their thermal behaviors of melting and freezing show characteristic features such as a wide pre-melting range and excessive supercooling and individual behaviors of single crystals even for the same substance. The melting temperatures of [bmim]Br and [bmim]Cl were determined from the broad DSC traces and discussed in relation to the crystal structure. We suggest that the observed characteristics are due to the dynamics of the cooperative change between gauche–trans (GT) and trans–trans (TT) conformations of the butyl group in the [bmim]<sup>+</sup> cation.

## 1. Introduction

Room-temperature ionic liquids have attracted much attention in applied chemistry as novel and green solvents. This is because of their advantages as solvents: thermal stability, nonvolatility, non-combustibility, amphiphilicity, and so on.<sup>1–5</sup> From the physicochemical viewpoint, one of the important questions is why their melting points are low despite their ionic characters. Investigation on thermal behaviors of ionic liquids, especially on the melting and freezing processes, would give us a clue to this question.

Thermal analyses on ionic liquids and their crystals have been performed by using differential scanning calorimetry (DSC), thermal gravity analysis (TGA), and so on.<sup>6–9</sup> They gave useful information regarding thermal properties of ionic liquids. In most of them, however, the experimental conditions were set such that the results were only preliminary. One of us constructed a super-high-sensitive apparatus of DSC with a baseline stability of  $\pm 3$  nW.<sup>10,11</sup> The apparatus is also designed to scan at a very slow rate (such as 0.01 mK/s) in both heating and cooling. In the present investigation, we studied the details of thermal properties of prototypes of ionic liquids by using this apparatus.

The samples used are 1-butyl-3-methylimidazolium chloride ([bmim]Cl) and its bromide ([bmim]Br). They are typical prototypes of ionic liquids, and their melting points are a little higher than room temperature. We chose them as the samples,

because their single crystals are available. Furthermore, we have their structural informations from recent X-ray diffraction studies<sup>12,13</sup> and characterization of isomers of the cation by Raman spectroscopy.<sup>14</sup> Our studies on the structures of [bmim]Cl by X-ray powder diffraction<sup>15</sup> showed that [bmim]Cl has two crystal forms, a monoclinic crystal (abbreviated as crystal (1) hereinafter) and an orthorhombic one (abbreviated as crystal (2)).<sup>16</sup> The difference between the two crystal structures originates from the rotational isomerism around the C7–C8–C9 of the [bmim]<sup>+</sup> cation (Figure 1). Namely, crystal (1) consists of the trans–trans (TT) conformation, and crystal (2) is composed of the gauche–trans (GT) one.<sup>12–15</sup> The crystal structure of [bmim]Br was also shown to be orthorhombic and isomorphic with crystal (2) of [bmim]Cl.<sup>13</sup> The recent study by Raman spectroscopy has shown that the two conformations of the [bmim]<sup>+</sup> ion coexist in the liquid state for both [bmim]Cl and [bmim]Br.<sup>14</sup> The structural features of these crystals and the liquids are summarized in Table 1. The present samples are known to be very hygroscopic. For this type of investigation, contamination by moisture must be avoided at all cost. To this end, we selected a single crystal of about 1 mm in size in dry N<sub>2</sub> and sealed hermitically into an aluminum vessel for the DSC specimen. Using a single crystal as the specimen was also important to prevent contamination.

As for the melting points for crystals (1) and (2) of [bmim]Cl, Holbrey et al.<sup>13</sup> reported the values determined by DSC. However, they did not describe the detailed experimental conditions. The melting temperature of [bmim]Br has also been reported recently.<sup>17,18</sup> As well as the melting temperatures of crystals (1) and (2) of [bmim]Cl and the crystal of [bmim]Br, we investigate their thermal properties, especially focusing on their melting and freezing behaviors.

<sup>†</sup> Part of the special issue "Physical Chemistry of Ionic Liquids".

<sup>\*</sup> Corresponding author. E-mail: k.nishikawa@faculty.chiba-u.jp.

<sup>‡</sup> Graduate School of Science and Technology.

<sup>§</sup> Center for Frontier Electronics and Photonics.

<sup>||</sup> Department of Chemistry, School of Science, The University of Tokyo.

<sup>⊥</sup> Department of Chemistry, The University of British Columbia.

<sup>#</sup> Faculty of Education.

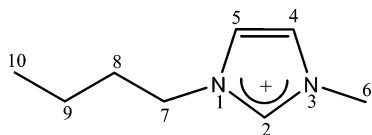


**Figure 1.** The structure of the [bmim]<sup>+</sup> cation and numbering for atoms.

**TABLE 1: Conformation of Butyl Group for [bmim]Cl and [bmim]Br**

	[bmim]Cl	[bmim]Br
crystal 1	monoclinic	
C7–C8–C9	TT	
crystal 2	orthorhombic	orthorhombic
C7–C8–C9	GT	GT
liquid	TT and GT	
C7–C8–C9		TT and GT

## 2. Experimental

By using thermal modules (TMs), one of us (K.T.) has developed a heat-flux-type DSC with a super-high sensitivity and a high resolution.<sup>10,11</sup> Its schematic drawing is shown in Figure 2. In Figure 2, TM3, TM4, and TM5 are used as heat pumps based on the Peltier effect. On the basis of the Zeebeck effect, TM1 and TM2, on which a sample and a reference are placed, work as detectors of the temperature difference between the heat sink and the sample or the reference. For the reference, we used an empty vessel. It is possible to carry out the measurements in either direction of heating or cooling. The temperature span measurable by this DSC is between 220 and 400 K, and the heat-flux ( $dQ/dt$ ) rate is from 3 nW to 1 W. The rate of cooling or heating is controllable in the range from 0.01 to 10 mK/s (from 0.036 to 36 K/h). The detail of the apparatus is given elsewhere.<sup>10,11</sup>

Under a dry N<sub>2</sub> atmosphere, [bmim]Cl or [bmim]Br were synthesized by mixing doubly distilled *N*-methylimidazole and 1-chlorobutane or 1-bromobutane in dry acetonitrile at room temperature, followed by gentle reflux. Single crystals of [bmim]Cl and the [bmim]Br were obtained by recrystallization from acetonitrile solutions. The conformation of the butyl group in the chloride crystals was identified by Raman spectroscopy. A single crystal was used as a specimen for each DSC measurement. The sample was transferred into an aluminum vessel and hermetically sealed in a globe box under dry N<sub>2</sub> atmosphere. The weights of the sample were typically 1 to 2 mg. The sample vessel was a commercially available aluminum one with a diameter of 4.5 mm and a depth of 1.8 mm. The standard heating or cooling rate of the present DSC measurements was 1 mK/s. To study the dependence of heating or cooling rate, the rate was changed from 0.1 to 2 mK/s.

## 3. Results and Discussion

The results on the crystal of [bmim]Br are first shown, followed by the ones of crystal (2) and crystal (1) of [bmim]Cl, because DSC traces become complex in that order.

**3.1. Crystal of [bmim]Br.** A single crystal of [bmim]Br, 2.09 mg in weight, was heated up to 360 K at a heating rate of 1 mK/s. At this temperature, the sample melted completely. The first trace of melting is not shown. As shown in Figure 3, the sample was then cooled at a cooling rate of 1 mK/s from 360 to 223 K and then heated at the same rate from 223 to 360 K. There was no thermal activity in the cooling process. In the heating process, however, two peaks were found; one is the exothermic peak at about 250 K, and the other is the endothermic peak at about 350 K. The former corresponds to freezing

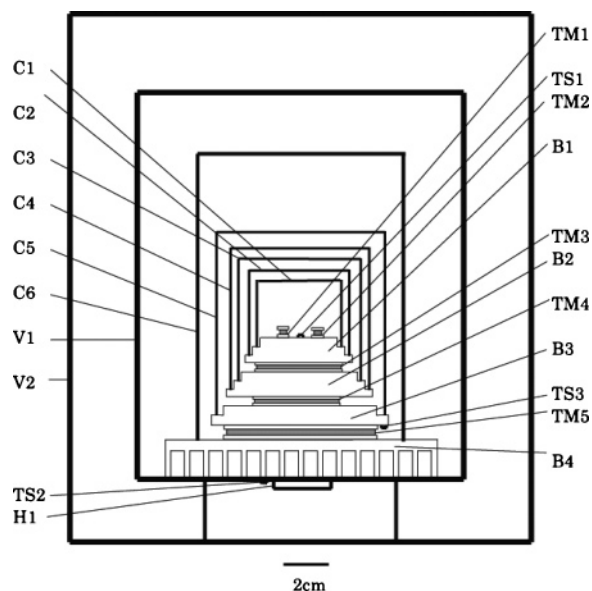


**Figure 2.** Schematic drawing of the homemade DSC with super-high sensitivity and resolution: TM, a thermal module; TS, a thermal sensor of Pt register; B, a base made of copper; H, a heater; C, a cap to make adiabatic circumstance; V, sample cell. The sample and the reference are set on TM1 and TM2, respectively.

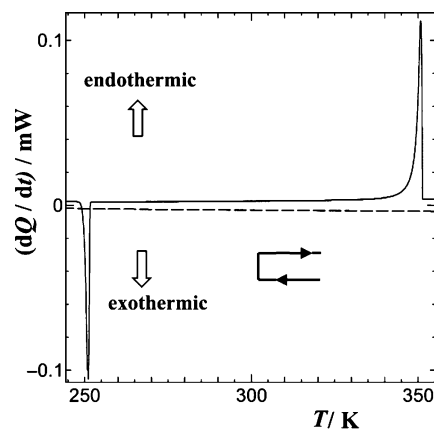


**Figure 3.** The DSC curves of [bmim]Br at the cooling and heating rate of 1 mK/s. The broken and solid traces refer to cooling and heating processes, respectively.

of the supercooled liquid and the latter to melting. This assignment is reasonable, because we find no exothermic peak when we start from a crystalline sample. We see the endothermic peak only after the appearance of the exothermic peak. Thus, the exothermic freezing peak appeared at about 100 K lower temperature than the melting peak. Stable existence of a supercooled state has been reported for many ionic liquids.<sup>6–8</sup> The present sample also shows this characteristic feature; namely, it is hard to crystallize. We repeated these measurements several times at the same cooling or heating rate. The DSC traces of melting were almost reproducible. Namely, for the same scanning rate, endothermic peaks appear in almost the same shapes at almost the same temperatures within  $\pm 0.1$  K, independent of thermal history or of specimen. On the other hand, the traces of freezing differ widely depending on the heating rate and the thermal history, which will be discussed later in this section.

From the following reasons, we consider the heating rate of 1 mK/s for this sample to be slow enough to keep almost quasi-static thermodynamic states. First, we turned back to the cooling process before reaching the top of the melting peak and cooled

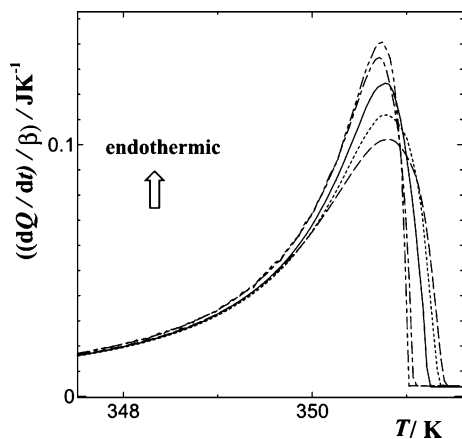


**Figure 4.** The magnified DSC curves for [bmim]Br around the melting peak with different heating rates: 2, 1, 0.5, 0.2, and 0.1 mK/s from the bottom to the top.

to 50 K below, and we then raised the temperature at the same heating rate. We observed that the DSC trace followed the same line within  $\pm 10$  nW. This shows that the pre-melting occurs in an almost quasi-static manner up to the top of the peak. Second, we also found by the Raman scattering experiment that the relaxation time to reach the equilibrium liquid state, where the proportion of the two conformers of the butyl group (see Table 1) is in equilibrium, is 5–6 min after instant melting.<sup>19</sup> The present heating rate is adequate enough to follow such slow dynamics.

We note that the melting peak is broad, ranging several K. This peak is too broad to regard this melting as a simple process. Our recent study on the melting of normal alkanes with long hydrocarbon chains showed that the width of the melting peak is only 0.1–0.2 K in the heating rate of 1 mK/s, using the same apparatus.<sup>20</sup> Rapid heating or cooling for a large amount of sample has been known to make the DSC trace broad because of the delay of heat transmission. In this experiment, however, the amount of the sample is very small and the heating rate is slow enough to mimic an almost quasi-static process as mentioned above. We thus suggest that this broadness is due to pre-melting, characteristic of the present sample. As shown in Table 1, [bmim]Br appears as only one crystal form in which the C7–C8–C9 conformation of the butyl group is in GT,<sup>13</sup> and both of GT and TT conformations coexist in liquid and supercooled liquid states.<sup>14</sup> As a result, a part of the cations must change the conformation from TT to GT at freezing and vice versa at melting. We considered that the pre-melting behavior is due to the increase of some fluctuation in the libration around the C–C bonds (especially C7–C8) within the potential minimum. This triggers the cooperative changes of conformation in the butyl chain and leads to melting.

We now turn to the melting temperature. In usual analyses of DSC, the point at which the deviation from the baseline starts is determined as the temperature of phase transition. However, we consider the usual determination to be inadequate in the present case, because the broad peak originates from the pre-melting characteristic of the internal motion of ions. Therefore, we defined the top of the peak as the melting point. The temperature determined in such a way is  $350.8 \pm 0.1$  K.

Next, we investigate heating-rate dependence on the melting trace. The five experiments in the heating rates of 0.1, 0.2, 0.5, 1, and 2 mK/s were performed for the same specimen. The results are shown in Figure 4. In order to make comparison independent of the heating rate, we convert the ordinate to the

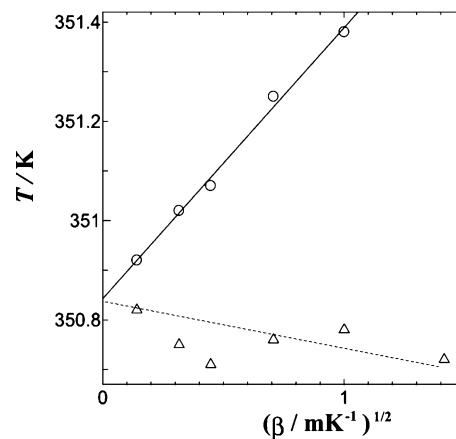


**Figure 5.** The break points of the melting peaks against the square-root of heating rates (○). The tops of the melting peaks are also shown (Δ).

values of apparent heat capacity ( $C$ ). It is given by dividing the heat flux ( $dQ/dt$ ) by the heating rate ( $\beta = dT/dt$ );

$$(dQ/dt)/(dT/dt) = dQ/dT = C \quad (1)$$

It is seen in Figure 4 that the peak of the trace becomes sharper as the heating rate becomes slower. The differences are conspicuous near the top of the melting trace and the downhill region past the top of the peak; the foot-hill of the lower temperature side of the top is almost the same. The high-temperature side of the peak drops sharply to the baseline, and thereafter, the baseline remains constant. Thus, there are no longer thermal processes after the sharp break in the slope. The temperatures of these breaks are plotted in Figure 5 against the square root of heating rate. Also plotted in the figure are the temperatures of the top of the melting peak. It is seen that the former forms a straight line. The melting point based on the transition theory of the square root of heating rate<sup>21</sup> is extrapolated as 350.8 K at zero heating rate. It is evident from Figure 5 that, by the measurement at the infinitely slow heating rate, the melting points determined from the top of the peak and from the break at the baseline would agree with each other. Namely, the top of the melting peak could be adopted as the approximate melting temperature within 0.3 K.

As for the melting temperature of [bmim]Br, Turner<sup>17</sup> and Paulechka<sup>18</sup> reported the values of  $347.5 \pm 0.8$  K (DSC) and 351.35 K (adiabatic calorimetry), respectively. As the main theme of the former study was not the thermodynamic analysis but the ab initio calculations,<sup>17</sup> it is thought that the attention for the treatment of the specimen was not so fine and the reported value might be approximate. The present value is 0.55 K lower than the value determined by adiabatic calorimetry.<sup>18</sup> We have paid attention in the different way from Paulechka so as to prevent contamination from mixing by use of a dry single crystal as the specimen. Although we cannot deny the mixing of a little water because of the high hygroscopic nature, we think that there was no contamination of unreacted materials or acetonitrile used for the solvent of reaction or recrystallization. Considering the differences of the methodology, the forms of the specimen and the specimen itself, it is possible to say that the present value of the melting temperature agrees with the data by Paulechka.<sup>18</sup>

The enthalpy changes of melting are listed in Table 2. These values were obtained by integration of the differences from a baseline. The baseline was drawn as a horizontal line at the value at 358 K. The values of enthalpy change systematically



TABLE 2: Enthalpy Changes at Melting

sample (weight)	heating rate (mK/s)	enthalpy change (kJ/mol)
[bmim]Br (2.09 mg)	0.1	$23.7 \pm 0.9$
	0.2	$23.5 \pm 0.9$
	0.5	$23.4 \pm 0.9$
	1.0	$23.4 \pm 0.9$
	2.0	$23.0 \pm 0.9$
[bmim]Cl (2)		
A (1.11 mg)	1.0	$21.5 \pm 1.0$
B (1.36 mg)	1.0	$18.5 \pm 1.0$
[bmim]Cl (1)		
a (0.76 mg)	1.0	9.3
b (1.91 mg)	1.0	14.5

and slightly become larger as the heating rate becomes slower. The convergent value is  $23.6 \pm 0.9 \text{ kJ mol}^{-1}$ , which is obtained by a least-square extrapolation. The present value agrees fairly well with the value of  $23.00 \pm 0.04 \text{ kJ/mol}$  determined by adiabatic calorimetry.<sup>18</sup> One of the origins of the difference seems to be the difference in the assignment of the starting point of the melting. As this sample is characterized by a wide pre-melting phenomenon, the region of integration may be somewhat arbitrary.

The enthalpy changes of melting for alkali bromides are reported to be 26.1 (NaBr), 26 (KBr), 15.5 (RbBr), and  $7.1 \text{ kJ mol}^{-1}$  (CsBr).<sup>22</sup> The value for [bmim]Br is almost equal to those of the inorganic salts with a very strong ionic bonding. It is known that  $\text{Br}^-$  ions do not form perfect ionic bonding with bulky [bmim]<sup>+</sup> ions with delocalized positive charge. In addition to the ionic interaction, we must consider the contribution of the conformation change, hydrogen bonding, and polar and nonpolar interactions. As shown in Table 1, a part of the [bmim]<sup>+</sup> ions must change the conformation of the butyl group from GT to TT for melting. For a free [bmim]<sup>+</sup> cation, it is reported from the ab initio calculations<sup>18</sup> that the energy difference of the TT conformation from the TG conformation is from  $-1.7$  to  $3.8 \text{ kJ mol}^{-1}$ ; the deviation of the values is due to the difference of the calculation levels. For the free cation, the energy difference between GT and TT conformers is little; however, it seems necessary to absorb the energy to change from GT to TT conformations in the crystalline field. From NMR studies,<sup>23</sup> it is well-known that the hydrogen atom (H2) bonding to C2 (Figure 1) is very protonic and has a strong tendency to form a hydrogen bond with an anion. Indeed, it is demonstrated by the structural determination of the single crystal that  $\text{Br}^-$  ions form strong hydrogen bonds with H2 hydrogen atoms.<sup>13</sup> If so, the large enthalpy of melting may partly be due to breaking of the hydrogen bonds.

The DSC traces for the crystallization from the supercooled liquid are shown in Figure 6. We note that this is a highly nonequilibrium dynamic process, unlike the melting process at about 350 K. Three trials were carried out at the heating rate of 1 mK/s. Each valley has two components. In Figure 6, the specimen at the lower temperature region than the valley is a supercooled liquid, in which both of the GT and TT conformers of the butyl group of a [bmim]<sup>+</sup> cation coexist.<sup>19</sup> On the other hand, [bmim]Br of the higher temperature region than the valley is in a crystal where only the GT conformer exists.<sup>13,19</sup> Taking into consideration the structural change of the cation mentioned above, we interpret that the observed split in the freezing valley is due to dynamics of crystallization. Namely, the [bmim]<sup>+</sup> cations with the GT conformation and  $\text{Br}^-$  anions crystallize at first, and the [bmim]<sup>+</sup> cations with the TT conformation form the crystal after changing the conformation from TT to GT. The lower-temperature component of the valley can be assigned

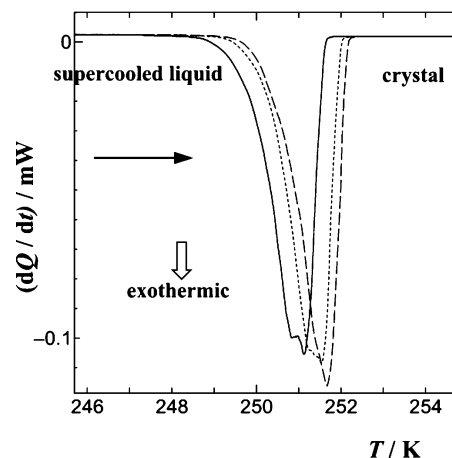


Figure 6. The magnified DSC curves for [bmim]Br around the freezing point from the supercooled liquid. All the experiments are carried out for the same sample and at the heating rate of 1 mK/s.

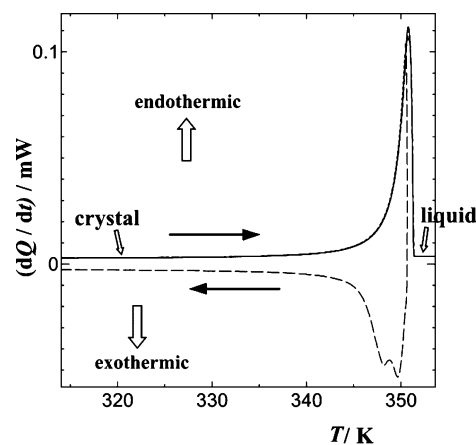
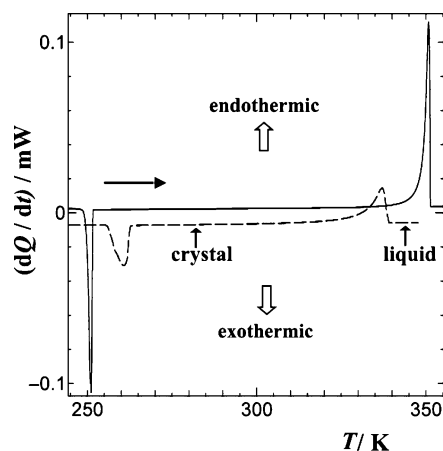


Figure 7. The magnified DSC curves for [bmim]Br around the melting point. The broken curve shows the trace where the sample is cooled on the way of the pre-melting process. The heating and cooling rates are 1 mK/s.

to the direct crystallization of GT conformers, and the component of the higher temperature to the crystallization of TT conformers after the change of conformation from TT to GT. Of course, these changes in the conformation must be cooperative to form crystals. A large number of cations must cooperatively change their conformations. As a result, the dynamics of crystallization of [bmim]<sup>+</sup> with the TT configuration is slow enough to be picked up separately.

We anticipate that the same change of the conformation occurs in the melting process. However, this does not mean that the two processes, the change in conformation and the crystallization or melting, are two separate equilibrium steps. Otherwise, there should also be two peaks in the trace of a semi-static heating run. We see instead a smooth though broad peak as shown in Figure 4. Indeed, when we reverse the heating process to cooling at about half-way through the pre-melting region and upset the semi-static steady state heating, we observe the split in the valley. Figure 7 shows the trace of the experiments, where the sample was first heated to the point in the pre-melting region (solid line) and then was cooled (broken line). The heating and cooling rates for the traces were 1 mK/s. As is evident in the figure, the division of the valley was also observed. This division is more remarkable for the sample that is heated up nearer to the top of the melting curve. Is this split of the exothermic valley also due to the dynamical relation of the two processes discussed above? If so, the valley of higher



**Figure 8.** The DSC trace on heating for crystal (2) of [bmim]Cl is shown by the broken curve. For comparison, the trace for [bmim]Br is also shown by the solid curve.

temperature is assigned to the direct crystallization of the portion that locally melts with GT conformers, and that of lower temperature corresponds to the crystallization of the portion with TT conformers after the change of conformation to GT.

The wide peak or valley might originate from the impurities. However, we deny this possibility for the following two reasons. First, we applied a single crystal as the specimen. As a result, there was little chance of contamination by chemical impurities. Second, we have performed preliminary simultaneous measurements of DSC and Raman scattering using our handmade apparatus and have observed that the conformational change of the butyl group in the [bmim]<sup>+</sup> occurs at the pre-melting process, and the ratio of the anion with the TT conformation increases when approaching the top of the melting peak. The decisive results of the simultaneous measurements will be reported in near future.<sup>24</sup>

We conclude that the complex thermal behavior including the wide-ranging pre-melting of [bmim]Br is attributed to the cooperative change between GT and TT conformations of the butyl group in the cation. Melting or freezing occurs linking with the change of the conformations of the cation.

**3.2. Crystal (2) of [bmim]Cl.** It is known that crystal (2) of [bmim]Cl is isomorphic with the crystal of [bmim]Br, and the conformation is in GT for the C7–C8–C9 in the butyl group.<sup>13,14</sup> The DSC measurements for crystal (2) of [bmim]Cl were also performed in the heating or cooling rate of 1 mK/s in the same procedures as the one of the crystal of [bmim]Br. Like [bmim]Br, no peak was found in the cooling process from the liquid state and two peaks appeared in the heating process. The trace of the heating process for the single crystal, whose weight is 1.11 mg (sample **A**), is shown in Figure 8, with the one of [bmim]Br for comparison.

Comparing with two traces, the shapes of the peaks are different from each other. Both the melting peak and the freezing valley of [bmim]Cl are notably broader, and it is more conspicuous that the freezing valley consists of two components. In the case of [bmim]Cl, two kinds of [bmim]<sup>+</sup> cations with GT and TT conformations coexist in the liquid state as in the case of [bmim]Br. The difference in the bromide and chloride is that [bmim]Cl has a polymorphism of crystals (1) and (2) as shown in Table 1. The cations with the TT and GT conformations crystallize as crystal (1) and crystal (2), respectively. This shows that, for the chloride, both TT and GT are stable in the crystalline states. The two components in the freezing valleys for crystal (2) seem to originate from the difference of freezing of the two conformations. The freezing process occurs in a

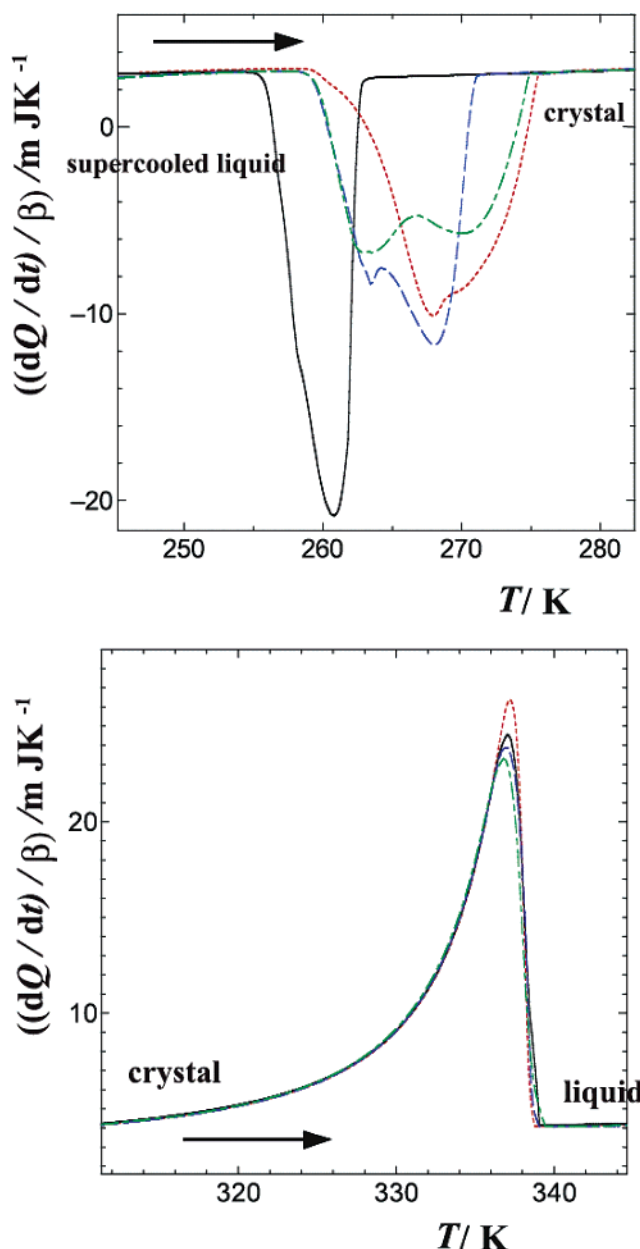


**Figure 9.** (a) The magnified DSC curves for crystal (2) of [bmim]Cl around the freezing point. The heating rates for the solid curve and others are 1 and 2 mK/s, respectively. (b) The magnified DSC curves for crystal (2) of [bmim]Cl around the melting point. The heating rates for the solid curve and others are 1 and 2 mK/s, respectively.

nonequilibrium manner after starting the transition. The freezing point depends crucially on thermal history as shown in Figure 9a, which shows the freezing traces for the same single crystal of [bmim]Cl and in the heating rates of 1 and 2 mK/s. It was an unexpected fact that the division of the freezing valley for a more rapid heating rate is more remarkable. This seems to show that the heating rate of 2 mK/s is more matched for the change of conformations between TT and GT. As for the melting process, if we start from the same single crystal of crystal (2), the melting occurs in the almost the same temperature even after it is melted and then frozen and even for different heating rates of 1 or 2 mK/s (Figure 9b).

As shown in Figure 10, however, the melting point shifts within 2 K dependent on the single crystal of crystal (2) of [bmim]Cl. The black curves refer to the single crystal **A** of 1.11 mg in weight as the starting sample, and the red curves to the single crystal **B** of 1.36 mg in weight. Both **A** and **B**

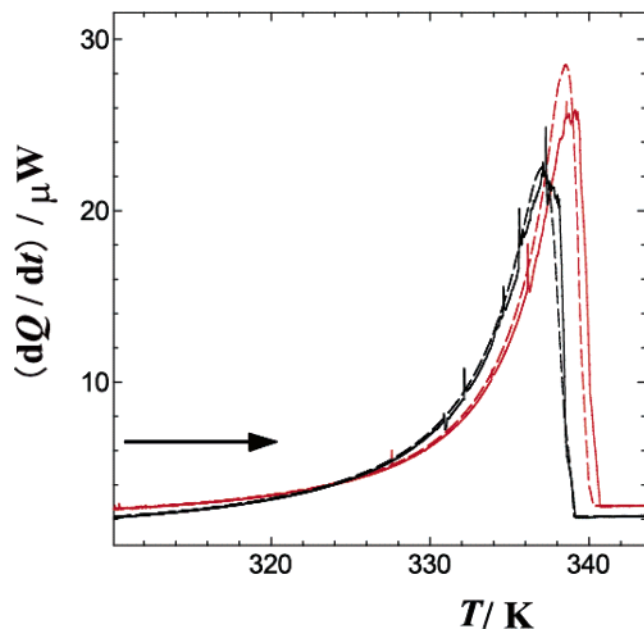


**Figure 10.** The magnified DSC curves for the single crystals of **A** (black curves) and **B** (red curves) for crystal (2) of [bmim]Cl around the melting point. The heating rate of all the runs is 1 mK/s.

were obtained in the same crystallization process. For **A** and **B**, the effect of thermal history on the melting curve was checked; namely, each sample was heated up to 350 K from the single crystal, kept as a liquid state during about 1 h, cooled down to 220 K, and then heated up 350 K. All the rates of heating and cooling were 1 mK/s. Some spikes appeared in the first run for each sample because of imperfect thermal contact between the sample and the vessel. It is surprising that the second trace of the melting follows almost the same trace of the first one for each sample, in spite of that each sample experienced melting and freezing. These experimental results show that the single crystal has the “character” and “memory”, which are kept in such an above-mentioned thermal history of the melting and freezing processes. These phenomena of the individual character and memory might be the impurities in the specimens. However, we selected a dry single crystal for each run. The specimens are pure in the extent of forming single crystals. We think that there was little contamination of unreacted materials or acetonitrile used as the solvent of reaction and recrystallization, although contamination of water cannot be denied. The Raman scattering study on the conformational change between TT and GT in the liquid state just after the melting suggested the very long relaxation time to reach the equilibrium state.<sup>19</sup> The observed “memory” seems to be due to the long relaxation in the cooperative change of the conformers. In this stage, we conclude that the melting point of crystal (2) of [bmim]Cl is  $338 \pm 1$  K, if we determine it by the peak top of the melting curve. The width of uncertainty corresponds to the difference of samples. In the paper after the recognition of the polymorphism, the melting point of crystal (2) of [bmim]Cl is reported to be 339 K.<sup>13</sup> This value is consistent with the present value.

The enthalpy changes of melting are listed in Table 2. For **A** and **B**, these values are 21.5 and 18.5 kJ/mol, respectively. It seems that, as well as for [bmim]Br, the melting and freezing of crystal (2) of [bmim]Cl occur accompanied by the conformational change between GT and TT of the butyl group. As a result, the enthalpies for the change of conformations are included in the enthalpies of the melting. As for [bmim]Br, the GT conformer is much more stable in the crystalline state and

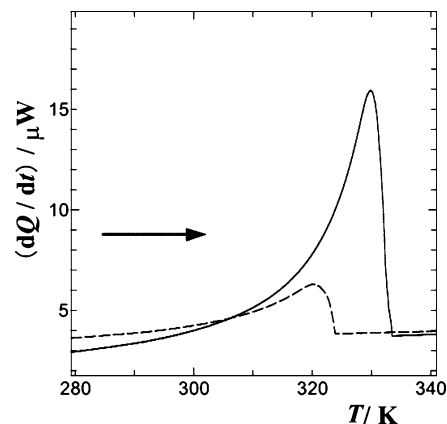


**Figure 11.** The magnified DSC curves for the single crystals of **a** (broken curve) and **b** (solid curve) for crystal (1) of [bmim]Cl around the melting point. The heating rate of all the runs is 1 mK/s.

it is supposed that most of the [bmim]<sup>+</sup> are crystalline as GT. On the other hand, it is provable that there are many defects in crystal (2) of [bmim]Cl. The defects are probably composed of amorphous components where the butyl chains do not marshal in the same conformation. In the X-ray diffraction patterns of powdered crystals of [bmim]Cl, broad patterns are detectable with the usual Bragg peaks.<sup>15</sup> This suggests the existence of noncrystalline parts even in the crystals. We conclude that the differences of the melting temperature and the enthalpy change are due to the defects.

The melting temperature of [bmim]Cl is lower than that of [bmim]Br, in contrast to the relation of usual chlorides and bromides. The known ionic radii of halide anions are as follows: Cl<sup>−</sup>, 1.81; Br<sup>−</sup>, 1.95. Because the radius of Br<sup>−</sup> is larger than that of Cl<sup>−</sup>, it is easily considered that the interaction of an anion and a cation of [bmim]Br is weak and the stability of [bmim]Br is low. This inference is observably contradicted with the data of the melting temperature obtained from the present study. As mentioned above, crystal (2) of [bmim]Cl is isomorphic with the crystal of [bmim]Br. In their crystals, Br<sup>−</sup> or Cl<sup>−</sup> anions are arranged in zigzag form in the channels formed by [bmim]<sup>+</sup> cations.<sup>12,13</sup> It is found that [bmim]<sup>+</sup> cations of [bmim]Cl and [bmim]Br are almost the same. It is guessed that the positive charges are delocalized in the imidazolium rings for the two crystals because the rings are not so much deformed from the regular pentagon. As a result, the Coulomb interactions of [bmim]<sup>+</sup> and Cl<sup>−</sup> are speculated to be almost the same as that of [bmim]<sup>+</sup> and Br<sup>−</sup>. The difference in the crystals is recognized in the distance between Cl<sup>−</sup> or Br<sup>−</sup> and the hydrogen bonded to C2, which we call the hydrogen H2. NMR studies show that H2 is the most protonic among the hydrogen atoms in [bmim]<sup>+</sup>.<sup>23</sup> The distance of Br–H2 is 0.245 nm, and the one of Cl–H2 is 0.256 nm.<sup>13</sup> Namely, the hydrogen bonding of Br–H2 is stronger than that of Cl–H2. It is thought that the size of the Br<sup>−</sup> anion is more fitted to form the strong hydrogen bonding with H2. This hydrogen bonding is supposed to originate the reverse of the melting temperature between the chloride and bromide.

**3.3. Crystal (1) of [bmim]Cl.** As for crystal (1) of [bmim]Cl, it was difficult to obtain reproducible DSC data. The patterns of DSC traces and melting temperatures of each single crystal are different individually. As an example, the melting peaks for two single crystals are shown in Figure 11. The single crystals were obtained in the same crystallization process. However, the melting temperature of crystal **a** (0.76 mg) and crystal **b** (1.91 mg) are 320 and 330 K, respectively, if we determine the temperature by the peak top of the melting curve.

Holbrey et al. reported that the melting temperature of crystal (1) is 318 K. The melting peaks are very broad, and it suggests a very complex pre-melting process. The enthalpy changes of the melting are 9.3 and 14.5 kJ/mol. It is surprising that the melting temperatures and enthalpy changes are so different. It is supposed that there are many more defects in crystal (1) compared with crystal (2).

#### 4. Concluding Remarks

We have studied the thermal properties of some prototypes of ionic liquids, i.e., those of [bmim]Br and [bmim]Cl, by using the super sensitive and high-resolution DSC, especially focusing on the melting and freezing processes. The [bmim]-based halogen ionic liquids are selected as the sample, because [bmim]<sup>+</sup> is a representative cation among ionic liquids. As the thermal behaviors of ionic liquids are generally complex, we have fixed the anions as halogens to study the properties of [bmim]<sup>+</sup> only. Moreover, crystal structures were determined, and Raman bands for some conformers of [bmim]<sup>+</sup> were assigned; they make it possible to elucidate the complex DSC traces. It is also noted that all the present experiments were carried out by using a respective single crystal. It is useful to avoid the mixing of chemical impurities or noncrystallized components as much as possible.

Each sample shows a long-ranged pre-melting phenomenon and a complex freezing behavior. These are attributed to the cooperative change between GT and TT conformers of the butyl group in the [bmim]<sup>+</sup> cation, linking to melting or freezing. These cooperative changes of the conformations are slow enough to be detected by the thermal analyses. It is concluded that the main origin that makes the thermal behaviors of [bmim]-based ionic liquids complex is the conformational change of the butyl group linking with the phase transitions. As for crystal (1) of [bmim]Cl, even a single crystal specimen seems to consist of two conformers with varying composition, so that the melting points are not reproducible depending on the composition. This entropic effect also has a large contribution to make the salts hard to crystallize.

**Acknowledgment.** The present study was supported by the Grant-in-Aid for Scientific Research (No. 17073002) in Priority Area "Science of Ionic Liquids" (Area Number 452) and by

the Grant-in-Aid for Scientific Research (No.17034010) in Priority Area "Molecular Nano Dynamics" (Area Number 432) from the Ministry of Education, Culture, Sports, Science, and Technology.

#### References and Notes

- (1) Welton, T. *Chem. Rev.* **1999**, 99, 2071.
- (2) Wasserscheid, P.; Klein, W. *Angew. Chem.* **2000**, 39, 3772.
- (3) Rogers, R. D.; Seddon, K. R. *Ionic Liquids—Industrial Applications for Green Chemistry*; ACS Symposium Series 818; American Chemical Society, Washington, DC, 2002.
- (4) Wasserscheid, P.; Welton, T., Eds. *Ionic Liquids in Syntheses*; VCH-Wiley: Weinheim, Germany, 2003.
- (5) Jessop, P. G.; Stanley, R. R.; Brown, R. A.; Echert, C. A.; Lietta, C. L.; Ngo, T. T.; Pollet, P. *Green Chem.* **2003**, 5, 123.
- (6) Holbrey, J. D.; Seddon, K. R. *J. Chem. Soc., Dalton Trans.* **1999**, 13, 2133.
- (7) Ngo, H. L.; LeCompte, K.; Hargens, L.; McEwen, A. B. *Thermochim. Acta* **2000**, 97, 357.
- (8) Huddleston, J. G.; Visser, A. E.; Matthew, W.; Willauer, H. D.; Broker, G. A.; Rogers, R. D. *Green Chem.* **2001**, 3, 156.
- (9) Marsh, K. N.; Boxall, J. A.; Lichtenthaler, R. *Fluid Phase Equilib.* **2004**, 219, 93.
- (10) Wang, S.; Tozaki, K.; Hayashi, H.; Hosaka, S.; Inaba, H. *Thermochim. Acta* **2003**, 408, 31.
- (11) Wang, S.; Tozaki, K.; Hayashi, H.; Inaba, H. *J. Therm. Anal. Calorim.* **2005**, 79, 605.
- (12) Saha, S.; Hayashi, S.; Kobayashi, A.; Hamaguchi, H. *Chem. Lett.* **2003**, 32, 740.
- (13) Holbrey, J. D.; Reichert, W. M.; Nieuwenhuyzen, M.; Johnston, S.; Seddon, K. R.; Rogers, R. D. *Chem. Commun.* **2003**, 1636.
- (14) Ozawa, R.; Hayashi, S.; Saha, S.; Kobayashi, A.; Hamaguchi, H. *Chem. Lett.* **2003**, 32, 948.
- (15) Hayashi, S.; Ozawa, R.; Hamaguchi, H. *Chem. Lett.* **2003**, 32, 498.
- (16) Our numbering for crystals (1) and (2) of the polymorphism is opposite to the one in ref 13. Just after our paper (ref 15), ref 13 was published. We adopt the numbering that was defined in our paper (ref 15).
- (17) Paulechka, Y. U.; Kabo, G. J.; Blokhin, A. V.; Shaplov, A. S.; Lozinskaya, E. I.; Vygodskii, Y. S. *J. Chem. Thermodyn.* <<http://dx.doi.org/10.1016/j.jct.2006.05.008>>.
- (18) Turner, E. A.; Pye, C. C.; Singer, R. D. *J. Phys. Chem. A* **2003**, 107, 2277.
- (19) Hamaguchi, H.; Ozawa, R. *Adv. Chem. Phys.* **2005**, 131, 85.
- (20) Wang, S.; Tozaki, K.; Hayashi, H.; Inaba, H.; Yamamoto, H. *Thermochim. Acta* **2006**, 448, 73.
- (21) Bonfiglioli, G.; Ferro, A.; Montalenti, G. *C. R. Reun. Annu. Commun. Thermodyn., Union Intern. Phys.* **1952**, 348.
- (22) Landolt-Boernstein, T. *Kalorische Zustandsgrossen*; Springer-Verlag: New York, 1961.
- (23) Headley, A. H.; Jackson, N. M. *J. Phys. Org. Chem.* **2002**, 15, 52.
- (24) Endo, T.; Tozaki, K.; Wang, S.; Shirota, H.; Nishikawa, K. In preparation.